Astron. Astrophys. 298, 711–725 (1995)

ASTRONOMY AND ASTROPHYSICS

Simultaneous and quasi-simultaneous observations of the continuum emission of the quasar 3C 273 from radio to γ-ray energies

G.G. Lichti[1], T. Balonek[2], T.J.-L. Courvoisier[3], N. Johnson[4], M. McConnell[5], B. McNamara[6], C. von Montigny[1,1], W. Paciesas[7], E.I. Robson[8], A. Sadun[9], C. Schalinski[10], A.G. Smith[11], R. Staubert[12], H. Steppe[13,2], B.N. Swanenburg[14], M.J.L. Turner[15], M.-H. Ulrich[16], and O.R. Williams[17]

[1]Max-Planck Institut für extraterrestrische Physik, Giessenbachstrasse, D-85748 Garching, Germany
[2]Department of Physiscs and Astronomy, Colgate University, Hamilton, NY 13343, USA
[3]Observatoire de Genève, Chemin des Maillettes 51, CH-1290 Sauverny, Switzerland
[4]Naval Research Laboratory, Washington DC 20375, USA
[5]University of New Hampshire, Institute for Studies of Earth, Oceans and Space, Durham, NH 03824, USA
[6]New Mexico State University, Las Cruces, NM 88003-0001, USA
[7]Department of Physiscs, University of Alabama, Huntsville AL 35899, USA
[8]School of Physics and Astronomy, University of Central Lancashire, Preston PR1 2HE, UK
[9]Bradley Observatory, Dptm. of Physics & Astrophysics, Agnes-Scott College, Decatur GA 30030, USA
[10]Institut für Radioastronomie im Millimeterbereich, Grenoble, France
[11]Department of Astronomy, University of Florida, Gainesville FL 32611, USA
[12]Astronomisches Institut der Universität Tübingen, Waldhäuser Str. 64, D-72076 Tübingen, Germany
[13]Institut für Radioastronomie im Millimeterbereich, Avda, Divina Pastora 7, E-18012 Granada, Spain
[14]Laboratory for Space Research Leiden, P.B. 9504, NL-2300 RA Leiden, The Netherlands
[15]Department of Physics, University of Leicester, Leicester LE17RH, UK
[16]European Southern Observatory, Karl-Schwarzschildstr. 2, D-85748 Garching, Germany
[17]Astrophysics Division, Space Science Departement of ESA/ESTEC, NL-2200 AG Noordwijk, The Netherlands

Received 20 July 1994 / Accepted 26 November 1994

Abstract. From June 15-28, 1991 the Compton Gamma-Ray Observatory (CGRO) observed the radio-loud quasar 3C 273. All four CGRO instruments detected radiation from this quasar in their relevant energy ranges (from 20 keV to 5 GeV). Simultaneous and quasi-simultaneous observations by instruments sensitive at other wavelengths have also been performed. The data from all these observations, spanning the frequency range from $5 \cdot 10^9$ Hz to $8.5 \cdot 10^{24}$ Hz, were collected and analysed. Details of the observations and an overall energy-density spectrum are presented. This spectrum shows three maxima, one in the infrared (IR), one in the UV and another one at low-energy γ-rays, the latter two having nearly the same strength of $3.1 \cdot 10^{46}$ erg/(s frequency decade) and $2.7 \cdot 10^{46}$ erg/(s frequency decade), respectively. At low-energy γ-rays a break around 1 MeV (= $2.418 \cdot 10^{20}$ Hz) in the energy-density spectrum is evident. The change of the spectral index between X- and γ-rays is $\sim$0.8. The implications of these simultaneous and quasi-simultaneous observations on some theoretical models are discussed.

Key words: gamma-rays: observations – quasars: individual (3C 273) – infrared: galaxies – ultraviolet: galaxies – radio continuum: galaxies – X-rays: galaxies

1. Introduction

The detection of more than 35 Active Galactic Nuclei (AGN) by EGRET (Fichtel et al. 1994) has called the attention of the scientific community to these exotic extragalactic objects whose nature is still not fully understood. In order to obtain a better understanding of the physical processes which power these sources, simultaneous observations across the electromagnetic spectrum are essential. We attempt here to gain some more insight into these physical processes by presenting the results of such a multiwavelength study. The basis for this study were data collected during an international campaign to observe 3C 273, the nearest and brightest quasar, at the same time at all wavelengths of the

Send offprint requests to: G.G. Lichti

[1] Present address: NASA/Goddard Space Flight Center, Greenbelt, Maryland 20771; NAS/NRC Resident Research Associate

[2] We devote this paper to Hans Steppe who died during its preparation by a tragic accident on June 30, 1993.

electromagnetic spectrum. These multifrequency observations were initiated by R. Staubert and most of the planned observations were carried out successfully (Staubert 1992). Only the observation by ROSAT was not possible because of technical problems with the satellite. The data from these observations were analysed and we present the results of this analysis here.

The detection of the quasars 3C 273/3C 279 by COMPTEL and EGRET (Hermsen et al. 1993; von Montigny et al. 1993) during the observation period no. 3 of the Compton Gamma-Ray Observatory (CGRO) sky survey stimulated the CGRO collaboration to investigate the multifrequency aspects of these two quasars. This paper deals only with 3C 273, whereas the paper by Hartman et al. (1994) concentrates on 3C 279. First preliminary results of this study have already been published by Lichti et al. (1994a) and Lichti et al. (1994b).

The redshift of z=0.158 puts 3C 273 at a distance of ~820 Mpc (for H_o a value of 60 (km/s)/Mpc and for q_0 a value of 0.5 is used throughout the paper) making it the nearest and, in the optical, brightest quasar in the sky. This source was detected in 1962 as a very bright double radio source (Schmidt 1963). One component was identified with the optical quasar, the other with the jet seen in the optical. In 1970 3C 273 was detected at X-rays (Bowyer et al. 1970) and some years later a high-energy γ-ray source coinciding with the position of 3C 273 was found by COS-B (Swanenburg et al. 1978). Its tentative identification with this quasar was later confirmed by Bignami et al. (1981). This quasar has also been extensively studied at all the other wavelengths of the electromagnetic spectrum during the last decade (Ulrich 1981; Bezler et al. 1984; Courvoisier & Ulrich 1985; Courvoisier et al. 1987; Ulrich et al. 1988; Courvoisier et al. 1990; Turner et al. 1990; Staubert 1991; Maisack et al. 1992; Robson et al. 1993). Since this singularly bright quasar shows all the characteristic features which are typical for high-luminosity quasars (an optical and a radio jet, superluminal motion, a UV and soft X-ray excess, a high γ-ray luminosity and a complex time variability at all wavelengths) it seems to be best suited to perform a multiwavelength study as presented here in order to learn more about the physical processes occurring in these objects. Such a study has been done once before on this quasar (Sadun 1992), specifically during an outburst, whose spectral evolution was followed for well over a year. However, that study did not have the benefit of high-frequency coverage, specifically in the X-ray and γ-ray regions.

2. The observations

All of the observations took place between May 1991 and October 1991. However, most of them were performed during or near to the time span when CGRO observed 3C 273 (from June 15 - 28, 1991). In the following sections the data are presented and details about the observations in the different wavelength regions are given.

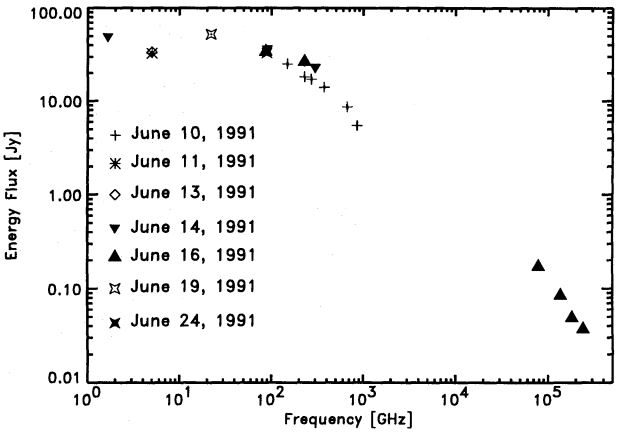

Fig. 1. Spectrum of radio, submm and infrared data (the errors are smaller than the fitting symbols)

2.1. At radio wavelengths

At radio wavelengths the bright quasar 3C 273 is often used as a calibration source and therefore it is quite regularly measured at different wavelengths by various radio telescopes. The measurements performed around the time of the CGRO observation are listed in Table 1.

During the CGRO observation period 3, VLBI observations were carried out by the 100 m radiotelescope at Effelsberg and 3C 273 was used as a calibration source, providing energy-flux measurements at wavelengths of 1.3 cm, 6 cm and 18 cm. These measurements were performed by I. Pauliny-Toth at 1.3 cm and 6 cm and by Witzel at 6 cm and 18 cm. Unfortunately only the measurements at 1.3 cm coincide with the CGRO observation, whereas the measurements at 6 cm and 18 cm took place shortly before it (from June 6 - 14, 1991).

At millimeter wavelengths 3C 273 is usually the strongest extragalactic point source and serves normally as a pointing calibrator for radio telescopes. For the energy-flux measurements performed with the 30m-MRT at Pico Veleta near Granada/Spain a 90 GHz Schottky receiver with a bandwidth of 500 MHz and a typical receiver temperature of 160 K was used. The few observations of 3C 273 performed in 1991 at 150 and 230 GHz were obtained with SIS receivers.

3C 273 was observed by cross scans through the source position consisting of 2 azimuth and 2 elevation subscans preceded by a calibration scan. After corrections for small pointing errors this observing procedure was repeated. 3C 273 was therefore calibrated in antenna temperature, corrected to outside the atmosphere. The conversion factor of antenna temperature to Jansky was determined using planets and/or a few galactic sources like compact HII regions (e. g. W3(OH) and NGC 7538) and planetary nebulae (e. g. NGC 7027 and K3-50A) which serve as secondary flux calibrators at the 30m-MRT. The energy fluxes measured in this way between end of May 1991 and end of October 1991 are shown in Table 1. The total errors given in this table consist of the square root of the quadratic sum of a scatter

Table 1. Observation summary of radio and submm data

date	TJD	wavelength	frequency [Ghz]	energy flux [Jy]	source of data	observatory
910614	8421	18 cm	1.66	47.8 ± 0.5	Witzel	Effelsberg
910606-910613	8413-8420	6 cm	4.99	33.5 ± 0.5	Pauliny-Toth	Effelsberg
910611	8418	6 cm	4.99	32.6 ± 0.5	Witzel	Effelsberg
910619-910623	8426-8430	1.3 cm	22.2	52 ± 0.9	Pauliny-Toth	Effelsberg
910624	8431	3.35 mm	89.6	33 ± 2	Balonek	NRAO Kitt Peak
910625	8432	3.35 mm	89.6	33 ± 2	Balonek	NRAO Kitt Peak
910626	8433	3.35 mm	89.6	33 ± 2	Balonek	NRAO Kitt Peak
910616	8423	3.33 mm	87	33.86 ± 0.1	Courvoisier	Metsähovi
910531	8407	3.33 mm	90	33.93 ± 1.71	Staubert	Pico Veleta
910610	8417	3.33 mm	90	33.65 ± 1.824	Staubert	Pico Veleta
910611	8418	3.33 mm	90	35.70 ± 1.79	Staubert	Pico Veleta
910614	8421	3.33 mm	90	35.31 ± 1.774	Staubert	Pico Veleta
910725	8462	3.33 mm	90	35.95 ± 1.8	Staubert	Pico Veleta
910903	8502	3.33 mm	90	42.06 ± 2.11	Staubert	Pico Veleta
910923	8522	3.33 mm	90	32.72 ± 2.774	Staubert	Pico Veleta
911024	8553	3.33 mm	90	29.30 ± 1.63	Staubert	Pico Veleta
911029	8558	3.33 mm	90	30.89 ± 2.27	Staubert	Pico Veleta
910725	8462	2.0 mm	150	27.54 ± 3.0	Staubert	Pico Veleta
910903	8502	2.0 mm	150	35.11 ± 3.54	Staubert	Pico Veleta
910610	8417	2.0 mm	150	25.07 ± 1.2	Robson	Mauna Kea
910610	8417	1.3 mm	230	18.16 ± 0.9	Robson	Mauna Kea
910611	8418	1.3 mm	230	28.24 ± 3.21	Staubert	Pico Veleta
910616	8421	1.3 mm	230	26.34 ± 2.652	Staubert	Pico Veleta
910610	8417	1.1 mm	272.5	17.16 ± 0.9	Robson	Mauna Kea
910614	8421	1.0 mm	300	22.3 ± 1.3	Staubert	Pico Veleta
910610	8417	0.8 mm	374.8	14.04 ± 0.7	Robson	Mauna Kea
910610	8417	0.45 mm	666.2	8.65 ± 0.5	Robson	Mauna Kea
910610	8417	0.35 mm	856.6	5.46 ± 0.6	Robson	Mauna Kea

error and a calibration error. The calibration error was assumed to be 5% at 90 GHz and 10% at 150 GHz and 230 GHz.

Observations at 89.6 GHz were obtained with the National Radio Astronomy Observatory's 12 m antenna on Kitt Peak using a two-channel (orthogonal linear polarizations) SIS receiver with a receiver temperature of ~60 K. Antenna pointing errors were determined using a standard five-point routine, followed by a sequence of ten on-off measurements to determine the source intensity. 3C 273 was observed two or three times each day. The compact HII region DR 21 and planets were used as flux-density calibrators, with calibration sources being observed every three to four hours to monitor temporal gain changes. These observations were obtained as part of an ongoing study by T. J. Balonek and W. A. Dent of the millimeter-wavelength time variability in radio-loud quasars.

3C 273 is regularly measured from 0.35 - 2 mm using the 15 m James Clark Maxwell Telescope on Mauna Kea, Hawaii, as part of a blazar monitoring campaign by I. Robson. Details of the observations and calibration techniques are found in Robson et al. (1993) and in the references therein. The observations were made on June 10, 1991 and the measured energy fluxes are shown in Table 1.

The 15 m Metsähovi radio telescope was used (in the frame of a regular radio monitoring) at 22 and 37 GHz. Calibrations were performed using the nearby 3C 274 source as described in Baars et al. (1977). A description of the equipment and the observing techniques can be found in Salonen et al. (1987).

2.2. *In the infrared*

In the infrared contemporaneous measurements in the near infrared (IR) region were performed on June 16, 1991 in the JHKL bands (at 1.25 μ, 1.65 μ, 2.2 μ and 3.8 μ) using the United Kingdom Infrared Telescope (UKIRT) on Mauna Kea as part of UKIRT observing for Robson's blazar monitoring program. During the measurements both telescopes were equipped with InSb detectors and with chopping secondaries. A summary of the observations in the infrared is given in Table 2.

In Fig. 1 the radio, submm and the infrared spectrum is shown for data collected between June 10 and June 24, 1991. At radio frequencies the spectrum is rather flat and steepens towards higher frequencies. It is obvious that the data in the submm and IR regimes cannot be fitted with a single power law. In the near IR the index α of a power law of the form $f_\nu \sim \nu^{-\alpha}$ has a value of ~1.37 whereas in the submm range it has a value of ~0.76. Similar values have been reported by Courvoisier et al. (1987) who concluded that the steepening around 5 μm (~$6 \cdot 10^4$ GHz) - also observed here - is a genuine feature of the source spectrum.

2.3. *In the optical*

At optical wavelengths only one simultaneous measurement exists at 4400 Å which was acquired by B. McNamara & G. Fitzgibbons on June 16 - 19, 1991. These differential observations were obtained using the New Mexico State University Blue Mesa Observatory's 24 inch reflecting telescope and photoelectric photometer. The photometer was equipped with a 1P21 photomultiplier and standard Johnson UBV filters. A

Table 2. Observation summary of infrared data

date	TJD	wavelength	frequency [Hz]	energy flux [mJy]	source of data	observatory
910616	8423	1.25 μ	$2.398 \cdot 10^{14}$	36.76 ± 0.2	Courvoisier	UKIRT Mauna Kea
910616	8423	1.65 μ	$1.817 \cdot 10^{14}$	48.64 ± 0.09	Courvoisier	UKIRT Mauna Kea
910616	8423	2.20 μ	$1.363 \cdot 10^{14}$	84.09 ± 0.62	Courvoisier	UKIRT Mauna Kea
910616	8423	3.80 μ	$7.889 \cdot 10^{13}$	171.5 ± 4.74	Courvoisier	UKIRT Mauna Kea

Table 3. Observation summary of optical data (energy-flux values have been corrected for interstellar absorption using a value for E_{B-V} of 0.03)

date	TJD	wavelength	frequency [Hz]	energy flux [mJy]	source of data	observatory
910601	8408	3439 Å	$8.718 \cdot 10^{14}$	36.75 ± 0.1	Courvoisier	Swiss Telescope in La Silla
910604	8411	3439 Å	$8.718 \cdot 10^{14}$	36.87 ± 0.2	Courvoisier	Swiss Telescope in La Silla
910601	8408	4003 Å	$7.489 \cdot 10^{14}$	35.69 ± 0.5	Courvoisier	Swiss Telescope in La Silla
910604	8411	4003 Å	$7.489 \cdot 10^{14}$	35.80 ± 0.1	Courvoisier	Swiss Telescope in La Silla
910601	8408	4213 Å	$7.116 \cdot 10^{14}$	34.84 ± 0.2	Courvoisier	Swiss Telescope in La Silla
910604	8411	4213 Å	$7.116 \cdot 10^{14}$	34.84 ± 0.3	Courvoisier	Swiss Telescope in La Silla
910602	8409	4360 Å	$6.876 \cdot 10^{14}$	27.4 ± 1.8	Smith	Rosemary-Hill Observatory
910616	8423	4400 Å	$6.818 \cdot 10^{14}$	36.9 ± 1	McNamara	Blue Mesa Observatory
910617	8424	4400 Å	$6.818 \cdot 10^{14}$	36.9 ± 1	McNamara	Blue Mesa Observatory
910618	8425	4400 Å	$6.818 \cdot 10^{14}$	36.9 ± 1	McNamara	Blue Mesa Observatory
910619	8426	4400 Å	$6.818 \cdot 10^{14}$	36.9 ± 1	McNamara	Blue Mesa Observatory
910523	8399	4400 Å	$6.818 \cdot 10^{14}$	35.9 ± 1.0	Sadun	Lowell Observatory
910524	8400	4400 Å	$6.818 \cdot 10^{14}$	36.6 ± 1.0	Sadun	Lowell Observatory
910525	8401	4400 Å	$6.818 \cdot 10^{14}$	36.4 ± 1.0	Sadun	Lowell Observatory
910526	8402	4400 Å	$6.818 \cdot 10^{14}$	36.4 ± 1.0	Sadun	Lowell Observatory
910527	8403	4400 Å	$6.818 \cdot 10^{14}$	36.7 ± 1.0	Sadun	Lowell Observatory
910601	8408	4466 Å	$6.713 \cdot 10^{14}$	34.54 ± 0.1	Courvoisier	Swiss Telescope in La Silla
910604	8411	4466 Å	$6.713 \cdot 10^{14}$	34.65 ± 0.2	Courvoisier	Swiss Telescope in La Silla
910601	8408	5395 Å	$5.557 \cdot 10^{14}$	35.66 ± 0.1	Courvoisier	Swiss Telescope in La Silla
910604	8411	5395 Å	$5.557 \cdot 10^{14}$	35.55 ± 0.7	Courvoisier	Swiss Telescope in La Silla
910601	8408	5479 Å	$5.472 \cdot 10^{14}$	35.83 ± 0.1	Courvoisier	Swiss Telescope in La Silla
910604	8411	5479 Å	$5.472 \cdot 10^{14}$	35.83 ± 0.2	Courvoisier	Swiss Telescope in La Silla
910523	8399	5500 Å	$5.455 \cdot 10^{14}$	33.3 ± 0.6	Sadun	Lowell Observatory
910524	8400	5500 Å	$5.455 \cdot 10^{14}$	33.9 ± 0.6	Sadun	Lowell Observatory
910525	8401	5500 Å	$5.455 \cdot 10^{14}$	33.6 ± 0.6	Sadun	Lowell Observatory
910526	8402	5500 Å	$5.455 \cdot 10^{14}$	33.1 ± 0.6	Sadun	Lowell Observatory
910527	8403	5500 Å	$5.455 \cdot 10^{14}$	33.4 ± 0.6	Sadun	Lowell Observatory
910601	8408	5798 Å	$5.171 \cdot 10^{14}$	35.80 ± 0.1	Courvoisier	Swiss Telescope in La Silla
910604	8411	5798 Å	$5.171 \cdot 10^{14}$	38.08 ± 0.1	Courvoisier	Swiss Telescope in La Silla
910523	8399	7000 Å	$4.286 \cdot 10^{14}$	29.6 ± 0.80	Sadun	Lowell Observatory
910524	8400	7000 Å	$4.286 \cdot 10^{14}$	30.4 ± 0.84	Sadun	Lowell Observatory
910525	8401	7000 Å	$4.286 \cdot 10^{14}$	30.3 ± 0.83	Sadun	Lowell Observatory
910526	8402	7000 Å	$4.286 \cdot 10^{14}$	30.7 ± 0.84	Sadun	Lowell Observatory
910527	8403	7000 Å	$4.286 \cdot 10^{14}$	30.4 ± 0.84	Sadun	Lowell Observatory
910523	8399	9000 Å	$3.333 \cdot 10^{14}$	29.6 ± 0.81	Sadun	Lowell Observatory
910524	8400	9000 Å	$3.333 \cdot 10^{14}$	33.6 ± 0.93	Sadun	Lowell Observatory
910525	8401	9000 Å	$3.333 \cdot 10^{14}$	29.7 ± 0.82	Sadun	Lowell Observatory
910526	8402	9000 Å	$3.333 \cdot 10^{14}$	29.8 ± 0.82	Sadun	Lowell Observatory
910527	8403	9000 Å	$3.333 \cdot 10^{14}$	30.0 ± 0.82	Sadun	Lowell Observatory

sequence of nearby reference stars in the field of 3C 273 was established using standard UBV stars from the lists of Crawford et al. (1971) and Landolt (1973). During each night differential measurements of 3C 273 were performed with respect to at least three of these secondary standards. Multiple integrations were obtained such that the error based upon photon statistics was less than 0.01 magnitudes. During the entire time interval over which these measurements were performed, no erratic

optical variations were noted from 3C 273. Magnitudes were converted into energy fluxes using the transformation given in Henden & Kaitchuck (1982). 3C 273 was observed by A. Smith on June 3, 1991 with the 76 cm Tinsley reflecting telescope of the Rosemary Hill Observatory using a Kodak 103a-O plate with a 2 mm Schott GG-13 glass filter which corresponds very well to the Johnson B-filter. The magnitudes during this observation were determined by comparing 3C 273 with a sequence of 10-12 comparison stars for which photoelectric magnitudes have been measured. The observation was reduced using the photoelectric sequence of Penston et al. (1971) and was finally corrected for atmospheric and interstellar extinction (see Table 7). The corrected magnitude has a value of 13.03 $\pm$ 0.07 and the corresponding energy flux value is listed in Table 3.

Broad-band photometric measurements (CCD imaging) using the B, V, R and I filters were performed with the Lowell Observatory's 42-inch telescope by A. Sadun about three weeks before the γ-ray measurements. The measured magnitudes were corrected for interstellar extinction and then transformed to physical energy-flux units (Jy) which are also given in Table 3. Details about the filter characteristics and the transformation are given in Sect. 3 and Table 7.

Using the Swiss telescope on La Silla, 3C 273 was observed on June 1 and 4, 1991 in the U, B1, B, B2, V1, V and G bands and the corresponding results are given in Table 3.

2.4. *In the ultraviolet*

The quasar 3C 273 has been observed by IUE on numerous occasions since the launch of the satellite in 1978. In 1985 we started a systematic monitoring with one observation every two weeks during the two yearly time intervals when 3C 273 is observable with IUE, mid-December – mid-February and May – mid-June. One observation lasts 4 hours (1/2 shift of IUE) and usually consists of 2 spectra taken with each of the two cameras, the SWP covering the range 1150–2000Å and the LWP camera covering the range 1900–3200Å. One such observation of 3C 273 was performed on June 17, 1991 and four spectra of 30 minutes each were obtained, two with the SWP camera (SWP 41851 and 41852), and two with the LWP camera (LWP 20617 and 20618).

For the present multiwavelength study we give in Table 4 the values of the continuum energy flux in the two windows free of obvious lines, 1260–1325Å and 1680–1720Å centered at λ_{obs} = 1292Å and 1700Å , respectively. The error quoted is the quadratic mean of the intrinsic error of the measurement and a 10% error which is the estimated absolute calibration uncertainty of IUE. A reddening correction for galactic absorption of $E_{B-V} = 0.03$ was applied to these values (see Sect. 3).

Is there an appreciable internal reddening to be added to that value? The UV spectrum of 3C 273 shows a small break at $\lambda \sim$ 2200–2500Å which could be a sign of internal reddening. However, this break could have two other origins. It could be due to the presence of the strong Fe II blends in the UV and optical spectrum of 3C 273; the minimum of the Fe II pseudo continuum at 2500Å produces the observed break. Or it could be a break due to the presence of two black-body components at two different temperatures (Ulrich et al. 1988). We consider now that the small break in the continuum spectrum is most likely due to the Fe II pseudo continuum, and that there is no convincing evidence for internal reddening. For these reasons we take $E_{B-V} = 0.03$. With Seaton's extinction curve (Seaton 1979), the de-reddening correction factors at 1292Å and 1700Å are 1.289 and 1.243, respectively.

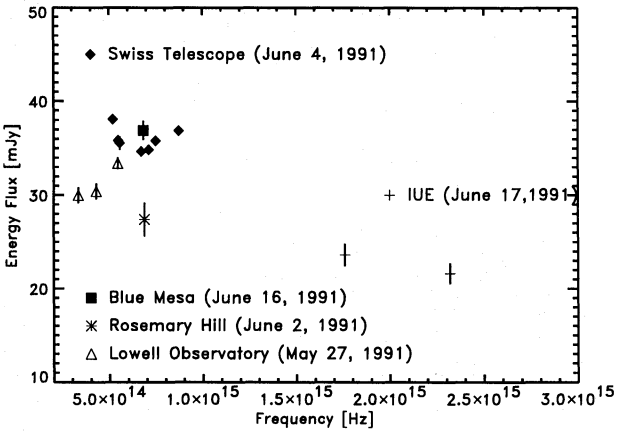

Fig. 2. Spectrum of 3C 273 at optical and UV frequencies (sometimes the errors are smaller than the fitting symbols)

The spectrum of the optical and the UV data is shown in Fig. 2. At optical freqencies a large scatter of the data is apparent which is very probably caused by variability effects. Nevertheless an increase of the energy flux with increasing frequency is observed at these frequencies reaching a maximum around 10^{15} Hz. At higher frequencies the energy flux decreases again.

2.5. *At X-rays*

At X-ray energies, 3C 273 was detected by both BATSE and OSSE. The SIGMA instrument on board of the GRANAT spacecraft observed 3C 273 on June 21/22 and 25/26, 1991; unfortunately, these data were not available for the present analysis. However, the Large Area Counters (LAC) on GINGA (Turner et al. 1989) observed and detected 3C 273 just prior to the CGRO observation at soft X-rays (from June 12-13, 1991). Due to the large 4000 cm^2 collecting area of the LAC, the spectrum of 3C 273 in the energy interval 1.65 - 31.35 keV could be measured with 40 narrow energy bins. The measured differential energy spectrum can be well represented by a power law of the form (90% errors are given)

$$F[\frac{photons}{cm^2 skeV}] = (2.33 \pm 0.04) \cdot 10^{-2} \cdot E_{keV}^{-(1.6\pm0.01)} \quad (1)$$

The reduced χ^2 of this fit to the data has a value of 1.2 for 43 degrees of freedom (goodness-of-fit probability = 21%; Lampton et al. 1976). But we want to mention that systematic effects

Table 4. Observation summary of UV data (energy-flux values corrected for interstellar absorption using a value for E_{B-V} of 0.03 and the reddening law of Seaton 1979)

date	TJD	observed wavelength	frequency [Hz]	energy flux [mJy]	source of data	observatory
910617	8424	1292 Å	$2.32 \cdot 10^{15}$	21.62 ± 1.1	Ulrich	IUE
910617	8424	1700 Å	$1.76 \cdot 10^{15}$	23.62 ± 1.2	Ulrich	IUE

due to possible attitude-control problems at this late phase in the GINGA mission have not been taken into account when fitting the spectrum. So the quoted errors may be underestimates! In Table 5, however, we present integrated photon fluxes for larger energy bins.

The GINGA errors quoted here exclude uncertainties due to problems with the attitude control during the last few months of its mission. The response of the LAC is an energy dependent function of the position of the source in the collimator field of view, giving rise to an apparent excess below 6 keV if sources are not observed on-axis. Corrections, based on scans of the Crab, have been applied to the data, but the systematic uncertainties in this procedure are not well known. However, we note that an analysis of data above 6 keV, which is unaffected, yields a similar result for the spectral index: $\alpha = 1.60 \pm 0.04$. A detailed discussion of this analysis will appear elsewhere.

The X-ray slope of 3C 273 as measured by EXOSAT and GINGA has been seen to vary over the last decade (Turner et al. 1990). It is worth noting that even considering the caveats expressed above, the GINGA spectrum reported here is the steepest measured by either instrument.

Using the Earth-occultation technique, BATSE was able to detect 3C 273 in the energy interval 20-320 keV at the $> 4\sigma$ level (Paciesas et al. 1994). This technique even allowed the derivation of a spectrum. The data in the energy interval 50 - 300 keV could be best described by a power law of the form

$$F[\frac{photons}{cm^2 skeV}] = (1.8 \pm 0.4) \cdot 10^{-5} \cdot (\frac{E}{100keV})^{-(1.57 \pm 0.24)} \quad (2)$$

Here the reduced χ^2 value of the fit was 0.94 for 40 degrees of freedom (goodness-of-fit probability = 55%).

OSSE detected 3C 273 at hard X- and low γ-rays (from 60 keV - 1.2 MeV) with a high significance ($\sim 35\sigma$) thus allowing the derivation of a spectrum with small energy bins (McNaron-Brown et al. 1994). The data (included in Table 5) in the energy range from 60 - 998 keV could be well fitted by a single power law of the form

$$F[\frac{photons}{cm^2 skeV}] = (4.7 \pm 0.2) \cdot 10^{-2} \cdot E_{keV}^{-(1.8 \pm 0.1)} \quad (3)$$

The reduced χ^2 value was 1.123 for 165 degrees of freedom (goodness-of-fit probability = 13.2%).

The BATSE spectrum (2) does not match very well the OSSE spectrum. But bearing in mind the large error the discrepancy is not significant. Comparing Eq. (1) and (3) one recognizes a slight steepening of the X-ray spectrum towards higher energies.

No evidence for emission of the 511 keV annihilation line was found by OSSE. Fitting a Gaussian with a power-law continuum to the data a line intensity of $0 \pm 2.4 \cdot 10^{-5}$ photons/(cm^2 s) was obtained. Upper limits for the 511 keV line emission from 3C 273 were derived for two cases: for a narrow line with a FWHM line width of 5 keV and for a broad line with a FWHM line width of 100 keV. The 99% confidence-level upper limits ($\chi^2 = 5.4$ for one interesting parameter) are $3.2 \cdot 10^{-5}$ photons/(cm^2 s) and $7 \cdot 10^{-5}$ photons/(cm^2 s), respectively.

2.6. At γ-rays

At γ-ray energies above 1.2 MeV the sensitivity of OSSE was not high enough to detect 3C 273. Only upper limits on the source photon flux could be derived. However COMPTEL was sensitive enough to measure γ-rays and first preliminary results of this detection were published by Hermsen et al. (1993). The final values are available now and will be published by Wiliams et al. (1994). These final photon-flux values are listed in Table 6. COMPTEL detected 3C 273 in the energy interval 0.75 - 8 MeV with a probability of $\sim 2 \cdot 10^{-5}$ ($\sim 4.3\sigma$). In the high-energy interval (8-30 MeV) only an upper limit could be derived. Because of the rather high significance of the detection, Williams et al. (1994) were able to subdivide the energy interval 0.75 - 8 MeV in three subintervals for which they quote individual flux values. If one determines the parameters of a power law using these three data points one obtains the following expression:

$$F[\frac{photons}{cm^2 sMeV}] = (2.44 \pm 0.74) \cdot 10^{-4} \cdot E_{MeV}^{-(1.96 \pm 0.44 \atop 0.27)} \quad (4)$$

This is in agreement with the spectrum (3) measured by OSSE. The reduced χ^2 value has a value of 0.107 for 1 degree of freedom (goodness-of-fit probability $\approx 75\%$).

Preliminary results from the observation of 3C 273 with EGRET in the energy range 70 MeV - 5 GeV were reported by von Montigny et al. (1993). The final results on this source are in preparation and will be published elsewhere. The data of this observation could be well described by a power law of the form

$$F[\frac{photons}{cm^2 sMeV}] = (3.0 \pm 1.7) \cdot 10^{-4} \cdot E_{MeV}^{-(2.39 \pm 0.13)} \quad (5)$$

The reduced χ^2 value was 1.2 for 2 degrees of freedom (goodness-of-fit probability = 32%).

A differential energy spectrum of 3C 273 from X- to γ-ray energies (from ~ 2 keV to ~ 1 GeV) is shown in Fig. 3. It reveals

Table 5. Observation summary of X-ray data. The mean frequencies were calculated using the relevant power laws

date	TJD	energy	mean frequency	photon flux	source of data	observatory
June 1991		[keV]	[Hz]	[$cm^{-2}\ s^{-1} keV^{-1}$]		
12-13	8419-8420	1.651-4	$6.174 \cdot 10^{17}$	$(6.38 \pm 0.132) \cdot 10^{-3}$	Turner, Williams	GINGA
12-13	8419-8420	4-8	$1.362 \cdot 10^{18}$	$(1.82 \pm 0.049) \cdot 10^{-3}$	Turner, Williams	GINGA
12-13	8419-8420	8-16	$2.725 \cdot 10^{18}$	$(6.0 \pm 0.212) \cdot 10^{-4}$	Turner, Williams	GINGA
12-13	8419-8420	16-31.352	$5.369 \cdot 10^{18}$	$(2.01 \pm 0.091) \cdot 10^{-4}$	Turner, Williams	GINGA
15-28	8422-8435	50-300	$2.91 \cdot 10^{19}$	$(1.2 \pm 0.31) \cdot 10^{-5}$	Paciesas	BATSE
15-28	8422-8435	60.44-71.55	$1.589 \cdot 10^{19}$	$(2.826 \pm 0.22) \cdot 10^{-5}$	Johnson	OSSE
15-28	8422-8435	71.55-82.68	$1.859 \cdot 10^{19}$	$(1.989 \pm 0.15) \cdot 10^{-5}$	Johnson	OSSE
15-28	8422-8435	82.68-93.78	$2.128 \cdot 10^{19}$	$(1.528 \pm 0.096) \cdot 10^{-5}$	Johnson	OSSE
15-28	8422-8435	93.78-104.9	$2.397 \cdot 10^{19}$	$(1.288 \pm 0.074) \cdot 10^{-5}$	Johnson	OSSE
15-28	8422-8435	104.9-121.4	$2.728 \cdot 10^{19}$	$(8.605 \pm 0.504) \cdot 10^{-6}$	Johnson	OSSE
15-28	8422-8435	121.4-143.5	$3.189 \cdot 10^{19}$	$(6.236 \pm 0.449) \cdot 10^{-6}$	Johnson	OSSE
15-28	8422-8435	143.5-165.6	$3.725 \cdot 10^{19}$	$(5.070 \pm 0.509) \cdot 10^{-6}$	Johnson	OSSE
15-28	8422-8435	165.6-187.6	$4.260 \cdot 10^{19}$	$(4.592 \pm 0.634) \cdot 10^{-6}$	Johnson	OSSE
15-28	8422-8435	187.6-215.1	$4.855 \cdot 10^{19}$	$(3.327 \pm 0.567) \cdot 10^{-6}$	Johnson	OSSE
15-28	8422-8435	215.1-248.1	$5.583 \cdot 10^{19}$	$(2.871 \pm 0.394) \cdot 10^{-6}$	Johnson	OSSE
15-28	8422-8435	248.1-419.8	$7.749 \cdot 10^{19}$	$(1.464 \pm 0.153) \cdot 10^{-6}$	Johnson	OSSE
15-28	8422-8435	419.8-714.7	$1.315 \cdot 10^{20}$	$(7.250 \pm 1.597) \cdot 10^{-7}$	Johnson	OSSE
15-28	8422-8435	714.7-1208.3	$2.232 \cdot 10^{20}$	$(1.688 \pm 1.135) \cdot 10^{-7}$	Johnson	OSSE

that the GINGA and OSSE data match very well although the measurements with the two instruments were not performed at the same time. This suggests that 3C 273 did not change its intensity at X-rays significantly between the two observations or it changed but then changed back to the previous level. This overall spectrum shows nicely the smooth and continuous steepening towards higher energies.

The data of this spectrum, excluding the BATSE data, can be well fitted by the following function:

$$F[\frac{photons}{cm^2 s MeV}] = (1.684 \pm 0.01) \cdot 10^{-3} \cdot \frac{(E/E_b)_{MeV}^{-(1.578 \pm 0.0015)}}{1 + (E/E_b)_{MeV}^{(0.80 \pm 0.03)}} \quad (6)$$

E_b has a value of (419.6 ± 1.5) keV. The reduced χ^2 value of this fit is 1.2 for 58 degrees of freedom (goodness-of-fit probability = 16%). The fit function reveals a steepening of the spectrum by ~0.8 for E >> 1 MeV.

2.7. *At ultrahigh-energetic γ-rays*

Between April 12 and May 14, 1991 3C 273 was observed with the Whipple High-Resolution Camera for 476 minutes on-source and 476 minutes off-source. The data of this observation were analyzed according to the procedure described in Reynolds et al. (1993). 3C 273 was not detected and therefore only an upper limit could be derived. For energies E> 0.55 TeV the 3σ photon-flux limit was $< 7.4 \cdot 10^{-12}$ cm^{-2} s^{-1}(M. A. Lawrence and T. C. Weekes, private communication). This upper flux limit was transformed into an upper limit of the energy density assuming an E^{-2} differential energy spectrum yielding a value of $6.512 \cdot 10^{-12} erg/(cm^2 s)$.

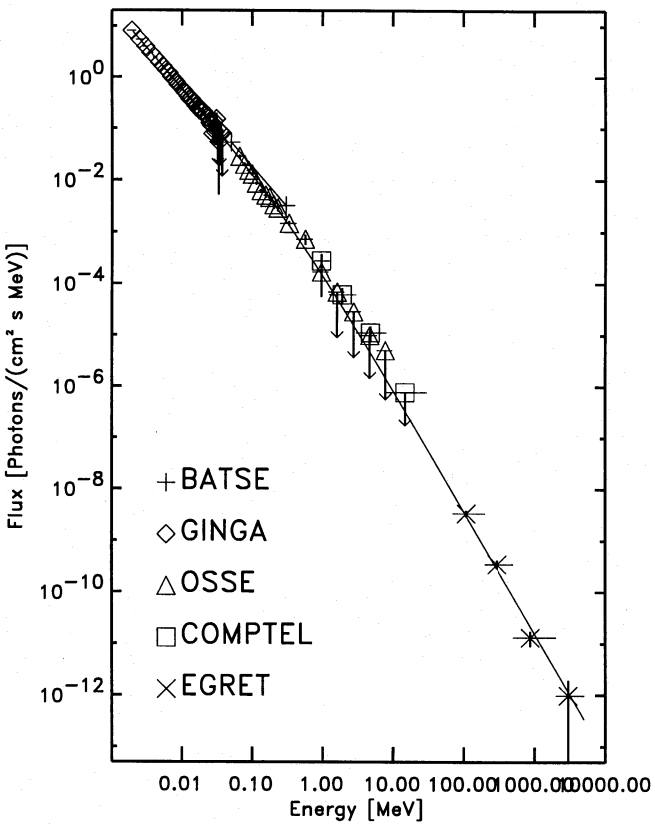

Fig. 3. Differential energy spectrum of 3C 273 from X- to γ-ray energies. The fit function (6) is plotted as a solid line

Table 6. Observation summary of γ-ray observations. The mean frequencies were calculated using the relevant power laws

date	TJD	energy	mean frequency	photon flux	source of data	observatory
June 1991		[MeV]	[Hz]	[$cm^{-2}\ s^{-1} MeV^{-1}$]		
15-28	8422-8435	1.208-2.046	$3.749 \cdot 10^{20}$	$< 6.9 \cdot 10^{-5}$	Johnson	OSSE
15-28	8422-8435	2.046-3.484	$6.410 \cdot 10^{20}$	$< 2.868 \cdot 10^{-5}$	Johnson	OSSE
15-28	8422-8435	3.484-5.894	$1.088 \cdot 10^{21}$	$< 9.951 \cdot 10^{-6}$	Johnson	OSSE
15-28	8422-8435	5.894-9.678	$1.818 \cdot 10^{21}$	$(1.223 \pm 3.835) \cdot 10^{-6}$	Johnson	OSSE
15-28	8422-8435	0.75 - 1.25	$2.326 \cdot 10^{20}$	$(27.6 \pm 9.6) \cdot 10^{-5}$	Williams	COMPTEL
15-28	8422-8435	1.25 - 3	$4.594 \cdot 10^{20}$	$(6.11 \pm 2.11) \cdot 10^{-5}$	Williams	COMPTEL
15-28	8422-8435	3 - 8	$1.157 \cdot 10^{21}$	$(1.12 \pm 0.38) \cdot 10^{-5}$	Williams	COMPTEL
15-28	8422-8435	8 - 30	$3.588 \cdot 10^{21}$	$< 7.73 \cdot 10^{-7}$	Williams	COMPTEL
15-28	8422-8435	70 - 200	$3.265 \cdot 10^{22}$	$(3.35 \pm 0.47) \cdot 10^{-9}$	von Montigny	EGRET
15-28	8422-8435	200 - 500	$8.464 \cdot 10^{22}$	$(3.48 \pm 0.68) \cdot 10^{-10}$	von Montigny	EGRET
15-28	8422-8435	500 - 2000	$3.023 \cdot 10^{23}$	$(1.32 \pm 0.43) \cdot 10^{-11}$	von Montigny	EGRET
15-28	8422-8435	2000 - 5000	$8.464 \cdot 10^{23}$	$(9.81 \pm 9.79) \cdot 10^{-13}$	von Montigny	EGRET

3. Data transformations and corrections

To allow a comparison of data measured with different instruments in different wavebands some transformations of the data are necessary. These transformations from the different units into a common energy-flux unit are not always straightforward and require a deep knowledge of the various instrument characteristics. In particular, the filter profiles from the various optical and IR telescopes differ slightly from each other. We have, therefore, taken great care that all these characteristics have been considered when transforming the measured magnitudes into energy fluxes. All magnitudes were corrected for interstellar extinction using the extinction law of Seaton (1979). For the reddening value in the direction to 3C 273 (l=289.89^0, b=64.352^0) a value of $E_{B-V} = 0.03$ was used. This value was derived from (a) the maps of Burstein & Heiles (1982) which give $E_{B-V} \approx 0.02$ and (b) from recent derived HI column densities N_H of $2 \cdot 10^{20} cm^{-2}$ (Stark et al. 1992) and $1.79 \cdot 10^{20} cm^{-2}$ (Dickey & Lockman 1990) using the relation $E_{B-V} = 1.5 \cdot 10^{-22} \cdot N_H$ of Bohlin et al. (1978) which yields for E_{B-V} values of 0.031 and 0.027, respectively. The corrections varied from ~0.05 (for the I-filter) to about 0.28 magnitudes (in the UV).

All quantities in this paper are expressed in the observers frame. The K-correction, which includes both the correction due to the observer seeing a different part of the intrinsic spectrum, depending on the redshift, and also the change in the observed bandwidth, has not been applied. Since, in this paper, we do not compare 3C 273 with objects at other redshifts its use is not required.

4. Time variability

If one wants to compare measurements which were not performed at the same epoch, variability can play an important role. Therefore time-variability aspects relevant in this respect will be addressed in this section.

At three radio frequencies (at 90, 150 and 230 GHz) 3C 273 was monitored for six years (from 1985-1991) using the 30 m telescope at Pico Veleta. During these observations three variable components were detected with time scales ranging from several weeks to several years (Steppe 1992). These are all much longer than the two weeks of the CGRO observation. These observations were continued in 1991 at 90 GHz (3.3 mm) and the corresponding time history is shown in Fig. 4. It is seen that the energy flux of 3C 273 was constant at the time of the CGRO observation (the observed variability during this time was less than 10%), but increased afterwards reaching a flat maximum in September (around TJD 8500). Then the intensity decreased again (the decrease even continued until the middle of 1992; Steppe, private communication). The time scale of these intensity variations is of the order of several weeks.

At the other wavelengths (1.3 mm, 2 mm, 1.3 cm, 3.3 cm, 6 cm and 18 cm) fewer data are available. But at 6 cm the intensity of 3C 273 was constant at a level of (33.5 ± 0.5) Jy from June 6-13, 1991 (TJD 8413-8420), i. e. shortly before the CGRO observation. Only on June 11, 1991 (TJD 8418) the measurement was performed a second time with the same instrument, but by a different observer (Witzel) leading to a slightly re-

Table 7. Filter characteristics for the 76 cm Tinsley telescope of the Rosemary-Hill Observatory (marked by *), of the Lowell Observatory's 42-inch telescope (marked by +) and of the Blue Mesa Telescope (marked by -). The magnitude corrections A_λ were calculated for an extinction value E_{B-V} of 0.03. log f are the observed flux values with these instruments and filters for a star with 0^{th} absolute magnitude

filter	λ [Å]	FWHM [Å]	log f [W $cm^{-2} \mu^{-1}$]	A_λ [mag]
UV	1292	-	-	0.277
UV	1700	-	-	0.234
B (*)	4360	950	-11.17	0.123
B (-)	4400	980	-11.143	0.122
B (+)	4400	980	-11.18	0.122
V (+)	5500	890	-11.42	0.095
R (+)	7000	2200	-11.76	0.069
I (+)	9000	2400	-12.08	0.047

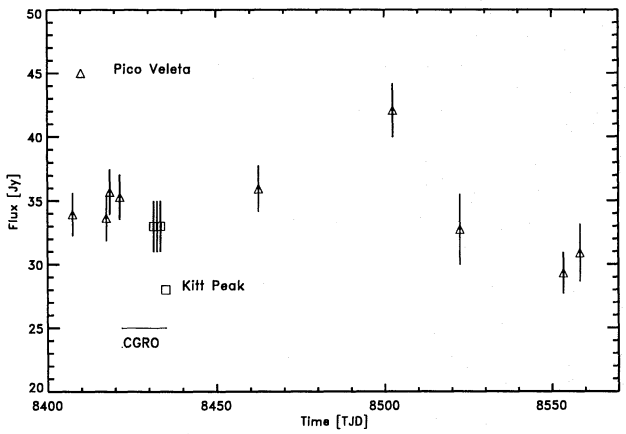

Fig. 4. Time history of radiodata at 3.3 mm (the time interval of the CGRO observation is indicated)

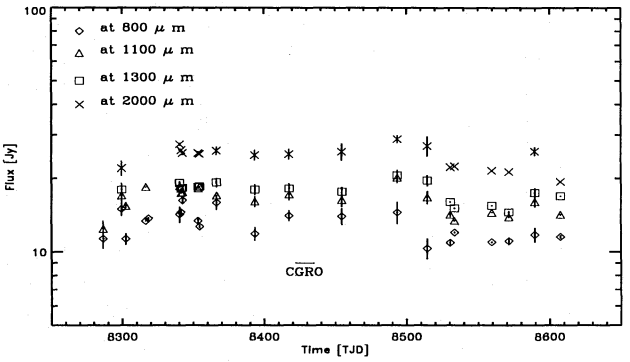

Fig. 5. Time variability of far infrared data (the time interval of the CGRO observation is indicated)

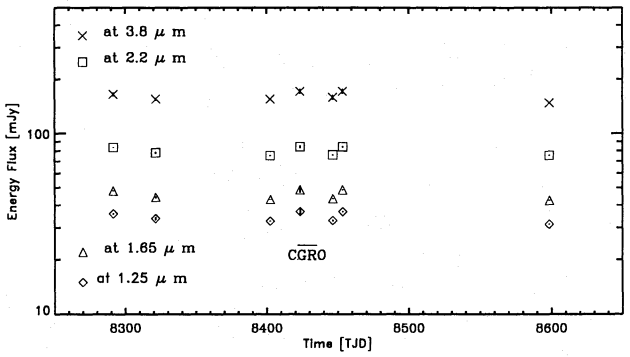

Fig. 6. Time variability of near infrared data

duced intensity (by ~2.7%). During October 1991 the source was again measured and had within the error still the same intensity (33.9 Jy; W. Reich, private communication). It seems therefore not unreasonable to assume that the source intensity during the CGRO observation was the same. This view is supported by earlier observations where a steady source intensity was observed at 1.3 cm from January 1984 till January 1985 (Courvoisier et al. 1987). However from 1986 till 1990 variations of the source energy flux up to 40% were observed at 1.3 cm and at 8.1 mm (Courvoisier et al. 1990). This shows that it is problematic to derive an energy-flux value based on interpolation. But from the doubling time (i. e. the time during which a source doubles its intensity) of ~0.5 years observed at radio wavelengths (see e. g. Robson et al. 1993), one can deduce that intensity variations are negligible on the time scale considered here. However short-term flaring activity has also been observed by the same authors and a similar behaviour cannot be excluded for the current observation.

The few observations at 150 GHz and at 230 GHz point to the fact that the maximum around TJD 8500 mentioned above occurred earlier or at least at the same time at higher frequencies. This could be a hint that optical-density effects play a role within the source region.

The time variability for the whole year 1991 for the far IR is shown in Fig. 5. The data points for the four shown wavebands scatter by less than 25%. Especially around the time interval when CGRO observed 3C 273, the energy fluxes did not change very much. Figure 6 shows the time variability of the near IR data. Here the scatter between the different data points is $<$ 15%, even less than in the far IR.

The doubling time in the IR is of the order of 10 months and therefore long-term variability does not play a role here. But again it should be remarked that short-term flaring activity (with time scales of 10 days and less) has been observed (Courvoisier et al. 1988). However, the coverage with IR data around the CGRO observation is good and no hints of such flaring activity are present in the data.

The time variability of the optical data is shown in Fig. 7. Within the statistical uncertainties the energy fluxes are constant for all wavelengths with two exceptions: at $\sim$ 4400 Å a significant decrease of the intensity was observed (from $\sim$ 36 mJy to $\sim$ 26 mJy) around June 3, 1991 (TJD 8410) and at 9000 Å a significantly (3.7σ) higher energy flux of (42.7 ± 1.2) mJy was observed on May 24, 1991 (TJD 8400). The origin of the sharp intensity decrease at 4400 Å is not known.

The intensity increase at about 9000 Å, however, is quite interesting since it occurs only in one filter and one can therefore assume that one is dealing with some kind of line-emission variability. The only line which could come into question and which is strong enough (1.42 mJy, Boggess et al. 1979) is the H_α line. But because the redshift-corrected wavelength of this line is at 7600 Å and because of the large widths of the R and I filters (2200 Å and 2400 Å, respectively) one should see the intensity change in both wavelength bands (with a higher intensity even in the R-band). Since this is not the case and since no significant line emission beyond the H_α line (i. e. towards longer wavelengths) is known (Sadun 1992) the intensity increase is very probably due to time variability of the continuum. The origin of this possible continuum-emission variability, however, is unknown.

It is worth mentioning that during the observations between May 23 -27, 1991 (TJD 8399-8403) with the Lowell Observa-

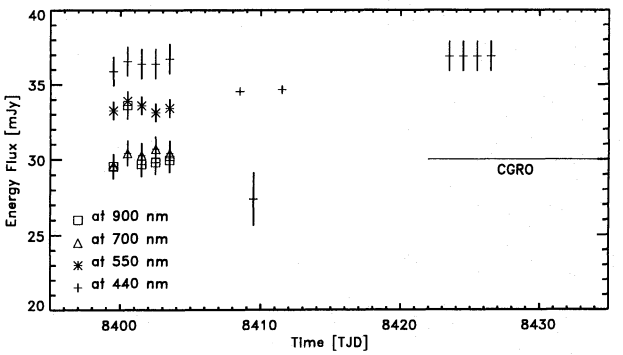

Fig. 7. Time variability of optical data (The time interval of the CGRO observation is indicated.) Note that the measurements were performed with different instruments! Note also that not all measurements around TJD 8410 were performed at exactly 440 nm (see Table 3)!

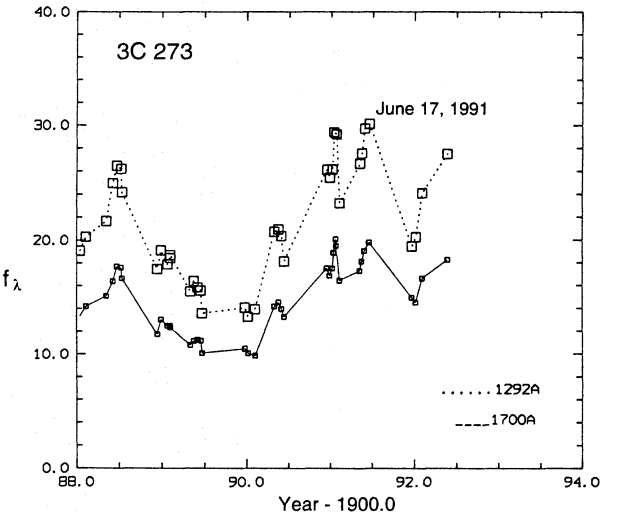

Fig. 8. Light curve of the continuum energy flux of 3C 273 at λ_{obser} = 1292Å and 1700Å. Abscissa: year minus 1900.0. Ordinates: f_λ (not corrected for reddening) in 10^{-14} erg cm^{-2} s^{-1} Å^{-1}

tory 3C 273 was about 0.3 magnitudes brighter than normal. It is also interesting to note that variability on a time scale of hours by ~0.1 magnitude was observed during these observations.

At optical wavelengths it is our experience that 3C 273 is a rather mild variable. In 17 years of monitoring by the Rosemary Hill Observatory only magnitude changes by 0.8 or less were observed. This contrasts dramatically with the magnitude changes of optically-violent variables which change their luminosity by 4 or 5 magnitudes. Nevertheless 3C 273 is capable of rapid flickerings by 0.5 to 0.75 magnitudes (Smith et al. 1993). Scanning the records of the Rosemary Hill Observatory revealed that changes by 0.3 magnitudes in 24 hours and 0.6 magnitudes in one week have been observed. So the energy-flux change between May 27 (TJD 8403) and June 3 (TJD 8410) observed at about 4400 Å (see Table 3 and Fig. 7) by ~0.3 magnitudes is not unusual.

The time history of the IUE observations of the last few years for two different UV wavelengths is shown in Fig. 8. At the time of the CGRO observations the continuum energy flux was at a maximum. The observation which was immediately preceding was performed on 27 May 1991 (at abscissa value 91.40) and the energy flux in the two continuum windows was the same within the error as the one measured on June 17, 1991 (91.46). The next observation after the one of June 17 was performed on 19 December 1991 (91.97) when 3C 273 was again observable with IUE. The energy flux was then at a minimum. As is apparent on Fig. 8, the energy flux variations of 3C 273 within any two weeks period do not exceed 10%. The energy flux during the CGRO observations can therefore be considered to have been constant within this limit and equal to the value on June 17.

The time variability of 3C 273 at X-rays is not well known. But Courvoisier et al. (1990) compiled a lightcurve of 3C 273 at X-rays using the data of EINSTEIN, EXOSAT and GINGA. During ten years of observation with poor sampling, intensity variations up to a factor of ~3 were observed. The fastest variation observed during this time span was a decrease by ~40% in 20 days (Courvoisier et al. 1987). This is of the same order as the time span of the CGRO observation, but from the facts that the GINGA observation took place only few days before the CGRO observation and matches the OSSE data well one can assume that our data are not affected by variability effects. But it should be remarked here that Ariel V has observed an X-ray flare with a time scale of < 1 day (Marshall et al. 1981).

Since the measurements at hard X-rays and at γ-rays were all performed simultaneously, time-variability effects do not play a role. But it should be remarked that at high γ-ray energies, intensity variations by a factor of ~4 within ~1 day were observed by EGRET for 3C 279 (Kniffen et al. 1993). Also other quasars were found by EGRET to be time variable, but normally on time scales of weeks to months (Fichtel 1993; Thompson et al. 1994).

A word of caution is in order here. In the energy-density spectrum shown below two different types of data are compared: the data at X- and γ-rays measured by CGRO are integrated over a period of two weeks whereas the data at longer wavelengths were measured on much shorter time scales (of the order of a day for GINGA or much less than that for the other observations). One has to bear this in mind when judging the result of this multiwavelength study as presented in the next section.

5. The energy-density spectrum

An energy-density spectrum for those data which were measured during the time span of the CGRO observation is shown in Fig. 9. Apart from the good coverage at γ-rays, the data are sparse and very little can be deduced from them. The only clear feature visible in this spectrum is a break at low γ-ray energies. The break energy appears to be around 5 MeV. This is not in agreement with the break energy E_b derived from the fit to the composite X-γ spectrum (see Eq. (6)). The discrepancy may be due to a little excess at low γ-ray energies which is not fitted well enough by the function (6).

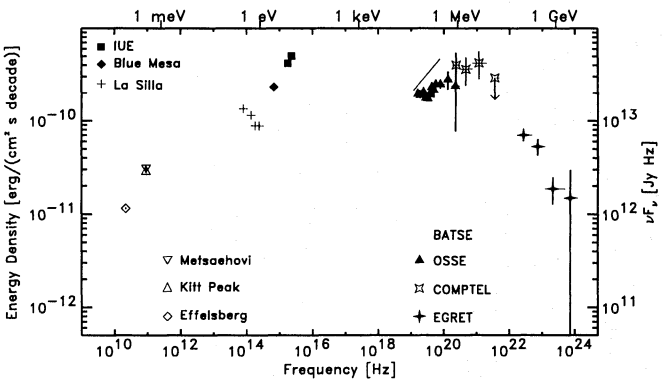

Fig. 9. Energy-density spectrum of simultaneous observations

Also remarkable is that the luminosity at γ-rays is approximately the same as in the UV. This is surprising because on September 28, 1981 the luminosity at hard X-rays was much higher than in the UV band where the latter had the same intensity as reported here (Bezler et al. 1984). The isotropic luminosity in the 20-200 keV band was $(1.2 \pm 0.12) \cdot 10^{47}$ erg/s. Integrating the composite spectrum (6) for the same energy interval one obtains only a luminosity per decade of frequency of $3.6 \cdot 10^{46}$ erg/s, nearly a factor of 4 less. A similar intensity difference was already recognized between the HEAO-A4 and the HEXE measurements (Primini et al. 1979; Bezler et al. 1984; Maisack et al. 1992). This points to a decoupling of the emission regions between the UV and X-rays and is in agreement with the findings of Courvoisier et al. (1990) who did not find a correlation between the UV and X-ray lightcurves.

Since the variability timescale of 3C 273 is normally of the order of a month and more (Courvoisier & Camenzind 1989) a quasi-simultaneous energy-density spectrum was constructed including data measured a few weeks around the CGRO observation (from May 27 - July 25, 1991). This spectrum is shown in Fig. 10 for the whole frequency range. A more complete picture emerges now. At radio frequencies a steep increase of the luminosity is observed reaching a first maximum around $6.7 \cdot 10^{11}$ Hz followed by a sharp cutoff. Due to missing data from $\sim 10^{12} - 8 \cdot 10^{13}$ Hz the shape of the cut-off remains unknown. The luminosity at maximum for isotropic emission amounts to $\sim 4.65 \cdot 10^{45}$ erg/s.

A second maximum - although not measured - must be reached in the near IR between 10^{13} and 10^{14} Hz. Then the energy density drops to a minimum around $2 \cdot 10^{14}$ Hz. The total isotropic luminosity at this frequency is $\sim 7 \cdot 10^{45}$ erg/s. From optical to UV the luminosity rises again reaching a maximum in the UV or at soft X-rays. The maximal luminosity reached here, probably associated with the hot component of the blue bump (Walter & Courvoisier 1992), has a value of $3.1 \cdot 10^{46}$ erg/s. No ROSAT data are available for June 1991 so that the link between the UV observations and the X-ray observations by GINGA is missing. Therefore, nothing can be said about the variable soft X-ray excess which was first detected with EXOSAT (Turner et al. 1985, 1990) and EINSTEIN (Masnou et al. 1992) and quantitatively measured by ROSAT (Staubert 1992).

At hard X-rays the energy density increases again until it reaches a maximum around 5 MeV (= $1.21 \cdot 10^{21}$ Hz) of $3.4 \cdot 10^{46}$ erg/s (slightly higher than the one reached in the UV). The maximum derived from Eq. (6), however, lies at a much lower energy of $\sim$480 keV. Again this points to an excess at low-energy γ-rays. Then the energy density drops rapidly towards higher energies.

6. Discussion

It is widely believed that AGNs are galaxies with a rotating supermassive black hole (a Kerr black hole) in their center which accretes matter from the surrounding forming an accretion disk. Currents flowing in the disk create a rotating magnetosphere according to the dynamo principle. The rotating magnetic fields create jets of plasma which are ejected from the central region perpendicular to the disk. Knots filled with plasma are accelerated along the jet axis to relativistic energies (Blandford & Königl 1979; Marscher 1980). The existence of these knots is known from VLBI measurements (Krichbaum et al. 1990; Bååth 1990).

This general picture seems to apply for 3C 273 as well as can be inferred from the following considerations. Ariel V has observed a significant change of the X-ray luminosity of 3C 273 in $\sim$1/2 day (Marshall et al. 1981). If one adopts the idea that the X- and γ-rays are produced by the same process (e. g. inverse Compton scattering) this implies a scale of $\sim 1.3 \cdot 10^{15}$ cm for the emission region. From the observed maximal γ-luminosity of $3.4 \cdot 10^{46}$ erg/s the compactness parameter $l = \frac{\sigma \cdot L}{mc^3 \cdot R}$ for 511 keV photons has a value of ~ 210 ($\sigma \approx 0.3 \sigma_T$). This high compactness would not allow the escape of the X-/γ-rays because of γ-γ absorption ($\tau_{\gamma\gamma} = \frac{l}{4\pi} \gg 1$; Herterich 1974). From the fact that X- and γ-rays have been observed and must therefore be able to escape the emission region one can derive a lower limit on the size of this region from the condition $\tau_{\gamma\gamma} \lesssim 1$. The emission region must therefore be larger than $\sim 1.5 \cdot 10^{16}$ cm. The proposed solution to this problem (Maraschi et al. 1992) is beaming of the X- and γ-rays.

An inspection of the energy-density spectrum of Fig. 10 shows at least three, if not four emission components. Each of these different components is produced by different emission processes. First, electrons moving in the magnetic fields emit synchrotron radiation which yields the spectrum observed in the radio and in the far IR. But also emission from dust contributes, especially in the IR. The fact that evidence for two maxima in the data at these low frequencies exists (one around $6.7 \cdot 10^{11}$ Hz and another one between $10^{13} - 10^{14}$ Hz) could be a hint for the existence of two electron populations with different bulk energies. It should be remarked, however, that the statistical significance of the first maximum is low ($\sim 2\sigma$). Therefore we do not claim that two electron populations exist! The prominent emission seen in the optical and in the UV (the big blue bump) is, in the case of 3C 273, predominantly emitted from a hot photosphere surrounding the accretion disk. The X- and γ-rays are

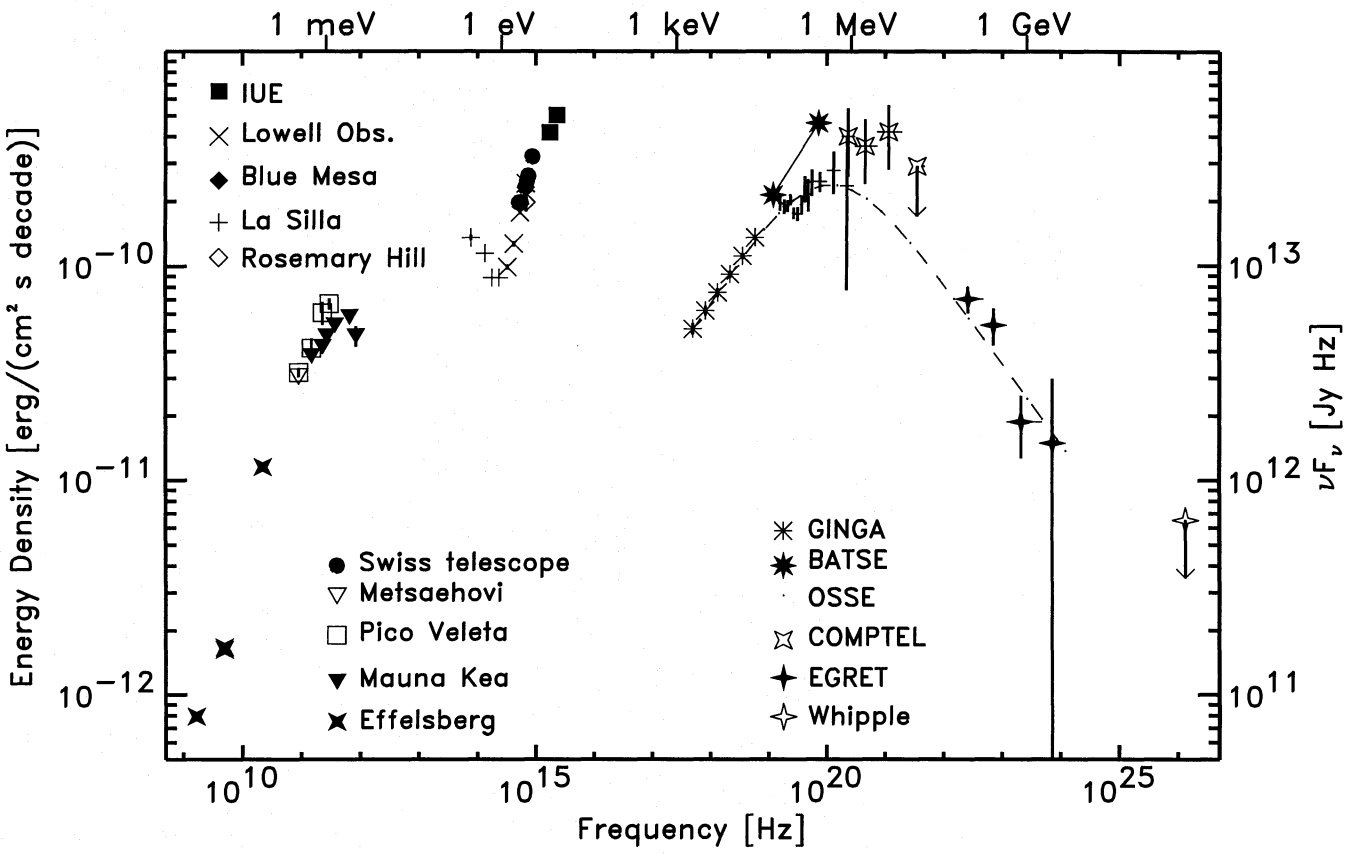

Fig. 10. Energy-density spectrum of 3C 273 of quasi-simultaneous observations. The fit of Eq. (6) is indicated by the dashed line

produced in optically thin regions by the inverse Compton process of relativistic electrons with the ambient synchrotron and/or optical and UV photons from the disk corona. The optically thin regions filled with relativistic electrons are associated with the superluminal knots observed at radio wavelengths. Models based on this scenario can explain the large-scale structure of the observed spectrum quite well. These models have also the advantage that they solve the luminosity problem because due to Doppler boosting, the radiation is highly beamed (for 3C 273 $\gamma \approx 10$ which leads to a reduction of the luminosity by a factor of $\sim 10^5$; Camenzind & Krockenberger 1992; Camenzind 1992).

Based on the sketched scenario many models have been proposed to explain the γ-ray emission from blazars. They can be distinguished into two different classes: the first one are models where the γ-rays are produced by leptons (mainly electrons and positrons) and the second one those were γ-rays are created by hadrons (mainly protons). The principal physical process of the lepton models is the inverse-Compton effect. Models based on this process were developed by Band & Grindlay (1986), Begelman & Sikora (1987), Zdiarski et al. (1990), Dermer et al. (1992), Dermer (1993), Zbyszewska (1993), Bloom & Marscher (1993), Sikora et al. (1994) and others. In the hadronic models the γ-rays are produced not only by leptonic, but also by hadronic interactions via the production of muons and pions which either decay directly into γ-rays or into electrons/positrons which then create the γ-rays. These processes were considered in the models of Sikora et al. (1987), Mannheim & Biermann (1989), Begelman et al. (1990), Bednarek & Calvani (1991) and Mannheim (1992, 1993). Some of these models will be considered in more detail in the following paragraphs.

Based on a leptonic model Dermer & Schlickeiser (1993) calculated an energy-density spectrum for 3C 273. This spectrum is compared with the data in Fig. 11 (solid line). Data from the ROSAT and IRAS observations of 3C 273, although not obtained simultaneously, have been added to the figure in order to close the gaps in the far IR and at soft X-ray energies (Staubert et al. 1992; Neugebauer et al. 1986). The observations with IRAS were performed during the year 1983 and the observations with ROSAT took place in December 1991. Whereas the γ-ray data are fitted reasonably well up to the highest energies it is obvious that the fit at X-rays is poor because the model predicts too high a luminosity. The model cannot explain a spectral softening significantly exceeding a value of 0.5 (the observations suggest a value of ~ 0.8). So the model does not explain the X-ray part of the spectrum and must be modified. Possible modifications could be consideration of additional energy losses like adiabatic losses and/or energy-dependent escape from the acceleration region which are not taken into account in the model. The theory models the UV bump from the accretion disk quite well whereas

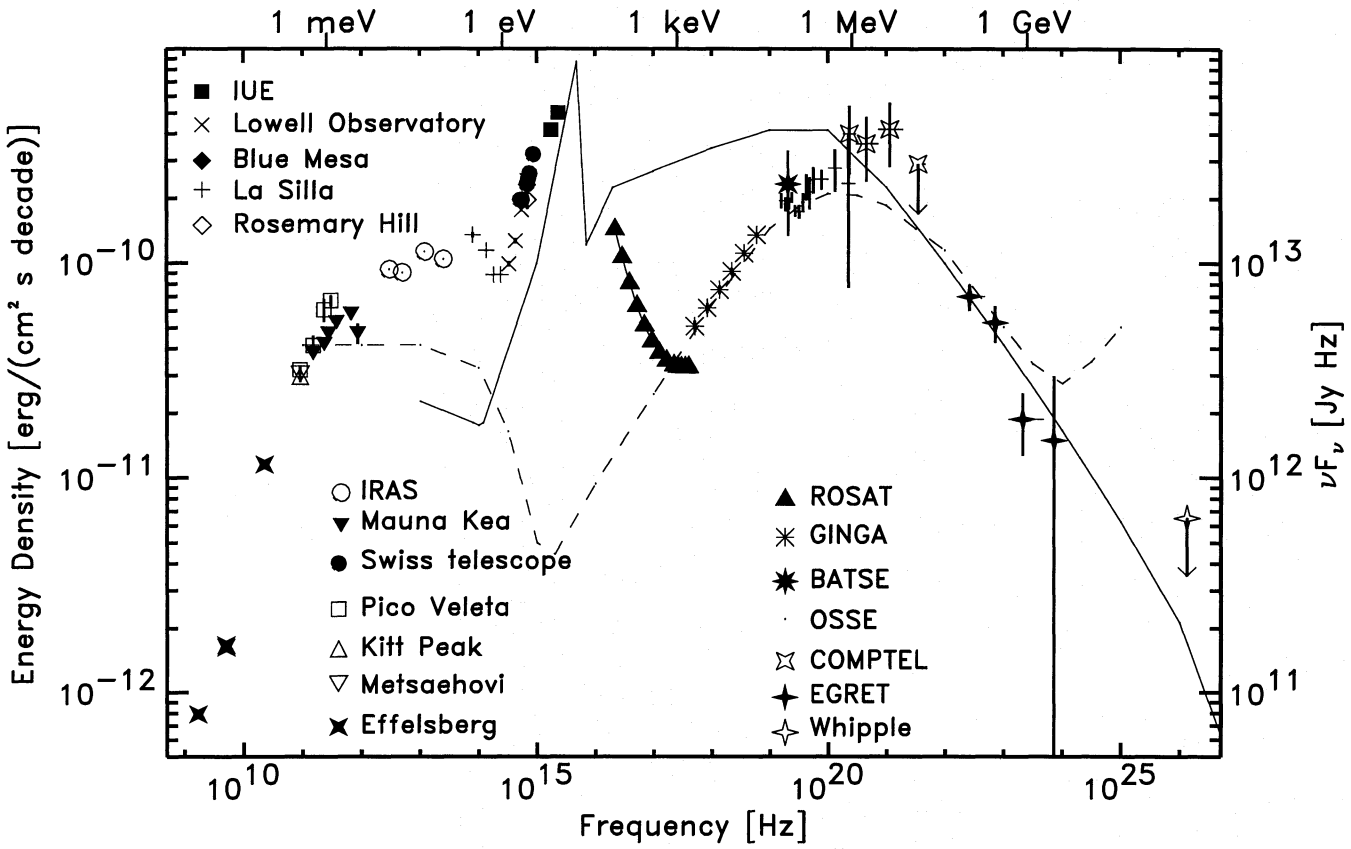

Fig. 11. Comparison of measurements with the inverse Compton model of Dermer & Schlickeiser (1993) (solid line) and with the proton-induced cascade model of Mannheim (1993) (dashed line). The IRAS data are from Neugebauer et al. (1986) and the ROSAT data from Staubert et al. (1992)

the fit to the optical data is poor because no fit to the radio data was attempted in this model calculation.

A similar model was recently developed by Sikora et al. (1994). The only difference to the previous model is a different source of the soft photons. Whereas in the model of Dermer & Schlickeiser (1993) these photons originate from the accretion disk they are produced in the new model close to the central engine and scattered back into the jet on a hot accretion-disk wind or on clouds of matter surrounding the jet. With this model the gross features of the energy-density spectrum of 3C 279 can be explained. But it seems not to be appropriate for 3C 273 because it is a "key prediction" of this model that the spectral break at γ-ray energies is ≈ 0.5. In the case of 3C 273, however, a significantly larger break of ≈ 0.8 is observed.

A model which can account for the observed break in the energy spectrum around $\sim$1 MeV is the two-flow model of Sol et al. (1989). In this model an e^+-e^- pair plasma is formed on the inner side of a subrelativistic outflow of an e^--p plasma from the accretion disk which is accelerated to relativistic energies via Alfvén turbulences (Henri & Pelletier 1991). The pairs of the e^--e^+ plasma suffer Compton cooling on the soft photons from the accretion disk thus producing the X- and γ-rays. The generated γ-rays can again produce e^+-e^- pairs by γ-γ interactions. This model has been used by Marcowith et al. (1994) to explain the spectral breaks observed in AGNs at γ-ray energies. According to this model "the break energy is equal to 511 keV blueshifted by the Doppler factor". For 3C 273 the Doppler factor is $\gtrsim 7$. The break energy should therefore be at energies $\gtrsim 3.5$ MeV. This is in agreement with the break energy at $\sim$5 MeV derived from the energy-density spectrum but not with the break energy at $\sim$420 keV derived from the fit to the data.

Another model in which electromagnetic showers induced by hadronic interactions of ultra-high energy protons with soft synchrotron photons in the jet are produced was investigated by Mannheim (1993). The spectrum of this model calculated for 3C 273 (and adapted at hard X-rays to non-simultaneous data of GINGA, HEXE and SIGMA) is also shown in Fig. 11 (dashed line). This model fits the X- and γ-rays reasonably well but it fails to explain the UV bump and the optical data because the model deals only with non-thermal processes. But at the maximum around $5 \cdot 10^{20}$ Hz the model predicts too low a luminosity ($\sim 1.6 \cdot 10^{46}$ erg/s instead of $2.3 \cdot 10^{46}$ erg/s) and around 10^{24} Hz its predictions are too high. Especially the hardening of the theoretical spectrum for frequencies $> 10^{24}$ Hz is a clear signature of this cascade model. The apparent conflict with the upper limit at 0.55 TeV ($\sim 10^{26}$ Hz), however, could be solved by tak-

ing into account in the model γ-γ absorption on the IR photons of the host galaxy. In this case the spectrum would break off rapidly around 10^{25} Hz, thus meeting the upper limit.

7. Conclusions

The discussion of the theoretical models reveals that they can explain in general the observed spectrum quite nicely but it also illustrates the limitation in our understanding of the emission processes of electromagnetic radiation in AGNs, because they are not able to explain all the observed features of the spectrum. So do some models not predict the large steepening of the spectrum at X- and γ-ray energies, others predict higher break energies than observed. The model in best agreement with the observed X- and γ-ray spectrum is the proton-initiated cascade model of Mannheim (1993). But also this model has to be improved if it aims for a perfect fit to the data. It is the hope that the unique data provided by this multiwavelength study will lead to better models which finally will help in gaining a better understanding of the physical processes which power these sources.

Acknowledgements. We thank I. Pauliny-Toth for supplying his radio data on 3C 273 and we are grateful to W. Reich for placing these data at our disposal. We also thank M. A. Lawrence and T. Weekes for giving the upper limit at ultra-high energies prior to publication. We want to thank all the persons who have performed the actual work at the observatories with specifically mentioning Dr. G. Fitzgibbons. The CGRO project has been supported by the German government through DARA grant 50 QV 9096, by NASA under grant NASA-26645 and by the Netherlands Organisation for Scientific Research (NWO), and the corresponding authors express their gratitude for this support.

References

Baars, J. W. M., R. Genzel, I. I. K. Pauliny-Toth, and A. Witzel, 1977, A&A 61, 99

Bååth, L. B., 1990, Proc. of the Workshop on Parsec-Scale Radio Jets (edts. J. A. Zensus and T. J. Pearson), Cambridge University Press, Cambridge, p. 91

Band, D. L., and J. E. Grindlay, 1986, ApJ 308, 576

Bednarek, W., and M. Calvani, 1991, A&A 245, 41

Begelman, M. C., B. Rudak, and M. Sikora, 1990, ApJ 362, 38

Begelman, and M. Sikora, 1987, ApJ 322, 650

Bezler, M., E. Kendziorra, R. Staubert, G. Hasinger, W. Pietsch, C. Reppin, J. Trümper, and W. Voges, 1984, A&A 136, 351

Bignami, G. F., K. Bennett, R. Buccheri, P. A. Caraveo, W. hermsen, G. Kanbach, G. G. Lichti, J. L. Masnou, H. A. Mayer-Hasselwander, J. A. Paul, B. Sacco, L. Scarsi, B. N. Swanenburg, and R. D. Wills, 1981, A&A 93, 71

Blandford, R. D., and A. Königl, 1979, ApJ 232, 34

Bloom, S. D., and A. P. Marscher, 1993, AIP Conf. Proc. 280, 578

Boggess, A., E. Daltabuit, S. Torres-Peimbert, F. B. Estabrook, H. D. Wahlquist, A. L. Lane, R. Green, J. B. Oke, M. Schmidt, B. Zimmerman, D. C. Morton, and R. C. Roeder, 1979, ApJ 230, L131

Bohlin, D. R. C., B. D. Savage and J. F. Drake, 1978, ApJ 224, 132

Bowyer, C. S., M. Lampton, J. Mack, and F. de Mendonca, 1970, ApJ 161, L1

Burstein, David, and Carl Heiles, 1982, AJ 87, 1165

Camenzind, M., 1992, Proc. of ISY Conf., Munich

Camenzind, M. and M. Krockenberger, 1992, A&A 255, 59

Courvoisier, T. J.-L. and M. Camenzind, 1989, A&A 224, 10

Courvoisier, T. J.-L. and M.-H. Ulrich, 1985, Nature 316, 524

Courvoisier, T. J.-L., M. J. L. Turner, E. I. Robson, W. K. Gear, R. Staubert, A. Blecha, P. Bouchet, R. Falomo, M. Valtonen, and H. Teräsranta, 1987, A&A 176, 197

Courvoisier, T. J.-L., E. I. Robson, A. Blecha, P. Bouchet, D. H. Hughes, K. Krisciunas, and H. E. Schwarz, 1988, Nature 335, 330

Courvoisier, T. J.-L., E. I. Robson, A. Blecha, P. Bouchet, R. Falomo, M. Maisack, R. Staubert, H. Teräsranta, M. J. L. Turner, E. Valtaoja, R. Walter, and W. Wamstecker, 1990, A&A 234, 73

Crawford, D. L., J. C. Golson, and A. U. Landolt, 1971, PASP 83, 652

Dermer, C. D., 1993, AIP Conf. Proc. 280, 541

Dermer, C. D., and R. Schlickeiser, 1993, ApJ 416, 458

Dermer, C. D., R. Schlickeiser, and A. Mastichiadis, 1992, A&A 256, L27

Dickey, J. M. and F. J. Lockman, 1990, ARA&A 28, 215

Fichtel, C. E., 1993, Proc. of the 16^{th} Symp. on Relativistic Astrophysics and of the 3^{rd} Symp. on Particles, Strings and Cosmology, Berkeley, December 1992

Fichtel, C. E., D. L. Bertsch, J. Chiang, B. L. Dingus, J. A. Esposito, J. M. Fierro, R. C. Hartman, S. D. Hunter, G. Kanbach, D. A. Kniffen, P. W. Kwok, Y. C. Lin, J. R. Mattox, H. A. Mayer-Hasselwander, L. McDonald, P. F. Michelson, C. von Montigny, P. L. Nolan, K. Pinkau, H.-D. Radecke, H. Rothermel, P. Sreekumar, M. Sommer, E. J. Schneid, D. J. Thompson, and T. Willis, 1994, ApJS 94, 551

Hartman, B. et al., in preparation

Henden, A. A., and R. H. Kaitchuck, 1982, Astronomical Photometry (van Nostrand Reinhold Company Inc., New York), p. 50

Henri, G., and G. Pelletier, 1991, ApJ 383, L7

Hermsen, W., H. J. M. Aarts, K. Bennett, H. Bloemen, H. de Boer, W. Collmar, A. Connors, R. Diehl, R. van Dijk, J. W. den Herder, L. Kuiper, G. G. Lichti, J. A. Lockwood, J. Macri, M. McConnell, D. Morris, J. M. Ryan, V. Schönfelder, G. Simpson, H. Steinle, A. W. Strong, B. N. Swanenburg, C. de Vries, W. R. Webber, O. W. Williams, and C. Winkler, 1993, A&A Suppl. Ser. 97, 97

Herterich, K., 1974, Nature 250, 311

Kniffen, D., D. L. Bertsch, C. E. Fichtel, R. C. Hartman, S. D. Hunter, G. Kanbach, P. W. Kwok, Y. C. Lin, J. R. Mattox, H. A. Mayer-Hasselwander, P. F. Michelson, C. von Montigny, P. L. Nolan, K. Pinkau, E. J. Schneid, P. Sreekumar, and D. J. Thompson, 1993, ApJ 411, 133

Krichbaum, T. P., R. S. Booth, A. J. Kus, B. O. Rönnäng, A. Witzel, D. A. Graham, I. I. K. Pauliny-Toth, A. Quirrenbach, C. A. Hummel, A. Alberdi, J. A. Zensus, K. J. Johnston, J. H. Spencer, A. E. E. Rogers, C. R. Lawrence, A. C. S. Readhead, H. Hirabayashi, M. Inoue, M. Morimoto, V. Dhawan, N. Bartel, I. I. Shapiro, B. F. Burke, and J. M. Marcaide, 1990, A&A 237, 3

Lampton, M., B. Margon, and S. Bowyer, 1976, ApJ 208, 177

Landolt, A. U., 1973, AJ 78, 959

Lichti, G. G., T. Balonek, T. J.-L. Courvoisier, N. Johnson, M. McConnell, C von Montigny, W. Paciesas, E. I. Robson, A. Sadun, C. Schalinski, A. G. Smith, R. Staubert, H. Steppe, B. N. Swanenburg, M. J. L. Turner, M.-H. Ulrich, and O. R. Williams, 1994a, Proc. of the IAU Symposium 159, edts. Courvoisier and Blecha (Kluwer Academic Publishers), 327

Lichti, G. G., C. von Montigny, T. Balonek, T. J.-L. Courvoisier, N. Johnson, M. McConnell, W. Paciesas, E. I. Robson, A. Sadun, C. Schalinski, H. Steppe, A. G. Smith, R. Staubert, B. N. Swanenburg, M. J. L. Turner, M.-H. Ulrich, and O. R. Williams, 1994b, Proc of the 2^{nd} Compton Symposium, AIP 304, edts. C. Fichtel, N. Gehrels and J. Norris (AIP Press), 611

Maisack, M., E. Kendziorra, B. Mony, R. Staubert, S. Döberei- ner, J. Englhauser, W. Pietsch, C. Reppin, J. Trümper, V. Efremov, S. Kaniovsky, A. Kusnetzov, and R. Sunyaev, 1992, A&A 262, 433

Mannheim, K., 1992, A&A 269, 67

Mannheim, K., 1993, Phys. Rev. D 48, 2408

Mannheim, K., and P. L. Biermann, 1989, A&A 221, 211

Maraschi, L., G. Ghisellini, and A. Celotti, 1992, ApJ 397, L5

Marcowith, A., G. Henri, and G. Pelletier, 1994, Proc. of the IAU Symposium 159, edts. Courvoisier and Blecha (Kluwer Academic Publishers), 347

Marscher, A. P., 1980, ApJ 235, 386

Marshall, N., R. S. Warwick, and K. A. Pounds, 1981, MNRAS 194, 987

Masnou, J. L., B. J. Wilkes, M. Elvis, J. C. McDowell, and K. A. Arnaud, 1992, A&A 253, 35

McNaron-Brown, K., J. E. Grove, W. N. Johnson, R. L. Kinzer, R. A. Kroeger, J. D. Kurfess, M. S. Strickman, D. A. Grabelsky, W. R. Purcell, M. P. Ulmer, G. V. Jung, and R. A. Cameron, 1994, in The Second Compton Symposium, ed. C. E. Fichtel, N. Gehrels, and J. P. Norris, AIP Conf. Proc 304, 587

Montigny, C. von, D. L. Bertsch, C. E. Fichtel, R. C. Hartman, S. D. Hunter, G. Kanbach, D. A. Kniffen, P. W. Kwok, Y. C. Lin, J. R. Mattox, H. A. Mayer-Hasselwander, P. F. Michelson, P. L. Nolan, K. Pinkau, H. Rothermel, E. Schneid, M. Sommer, P. Sreekumar, and D. J. Thompson, 1993, A&A Suppl. Ser. 97, 101

Neugebauer, G., G. K. Miley, B. T. Soifer, and P. E. Clegg, 1986, ApJ 308, 815

Paciesas, W. S., R. S. Mallozzi, G. N. Pendleton, B. A. Harmon, C. A. Wilson, S. N. Zhang, and G. J. Fishman, 1994, in The Second Compton Symposium, ed. C. E. Fichtel, N. Gehrels, and J. P. Norris, AIP Conf. Proc 304, 674

Penston, M. J., M. V. Penston, and A. Sandage, 1971, PASP 83, 783

Primini, F. A., B. A. Cooke, C. A. Dobson, S. K. Howe, A. Scheepmaker, W. A. Wheaton, and W. H. G. Lewin, 1979, Nature 278, 234

Reynolds, P. T., C. W. Akerlof, M. F. Cawley et al., 1993, ApJ 404, 206

Robson, E. I., S. J. Litchfield, W. K. Gear, D. H. Hughes, G. Sandell, T. J.-L. Courvoisier, S. Paltani, E. Valtaoja, H. Teräsranta, M. Tornikoski, H. Steppe, and M. C. H. Wright, 1993, MNRAS 262, 249

Sadun, A., 1992, J. Roy. Astr. Soc. Can. 86, 15

Salonen, E., H. Teräsranta, S. Urpo, M. Tiuri, I. G. Moiseev, N. S. Nesterov, E. Valtaoja, S. Haarala, H. Lehto, L. Valtaoja, P. Teerikorpi, and M. Valtonen, 1987, A&A Suppl. Ser. 70, 409

Schmidt, M., 1963, Nature 197, 1040

Seaton, M. J., 1979, MNRAS 187, 73P

Sikora, M., M. C. Begelman, and M. J. Rees, 1994, ApJ 421, 153

Sikora, M., J. G. Kirk, M. C. Begelman, and P. Schneider, 1987, ApJ 320, L81

Smith, A. G., A. D. Nair, R. J. Leacock, and S. D. Clements, 1993, AJ 105, 437

Sol, H., G. Pelletier, and E. Asséo, 1989, MNRAS 237, 411

Stark, A. A., C. F. Gammie, R. W. Wilson, J. Bally, R. A. Linke, C. Heiles, and M. Hurwitz, 1992, ApJS 79, 77

Staubert, R., 1992, Proc. of "X-Ray Emission from Active Galactic Nuclei and the Cosmic X-Ray Background", Garching, Germany, November 1991, MPE Report 235, 42

Staubert, R., H. Fink, T. Courvoisier, M.-H. Ulrich, H. Brunner, U. Zimmermann, E. Kendziorra, and K. Otterbein, 1992, AIP Conf. Proc. on "Testing the AGN Paradigma" (edts. S. S. Holt, S. G. Neff, C. M. Urry) 254, 366

Steppe, H., 1992, A&A 259, 61

Swanenburg, B. N., K. Bennett, G. F. Bignami, P. Caraveo, W. Hermsen, G. Kanbach, J. L. Masnou, H. A. Mayer-Hasselwander, J. A. Paul, B. Sacco, L. Scarsi, and R. D. Wills, 1978, Nature 275, 298

Thompson, D. J., D. L. Bertsch, B. L. Dingus, J. A. Esposito, C. E. Fichtel, R. C. Hartman, S. D. Hunter, P. Sreekumar, J. Chiang, J. M. Fierro, Y. C. Lin, P. F. Michelson, P. L. Nolan, G. Kanbach, H. A. Mayer-Hasselwander, C. von Montigny, H.-D. Radecke, D. A. Kniffen, J. R. Mattox, and E. J. Schneid, 1994, Proc. of the IAU Symp. 159, edts. Courvoisier and Blecha (Kluwer Academic Publishers), 49

Turner, M. J. L. T. Courvoisier, R. Staubert, D. Molteni, and J. Trümper, 1985, Space Sci. Rev. 40, 623

Turner, M. J. L., H. D. Thomas, B. E. Patchett, D. H. Reading, K. Mackishima, T. Ohashi, T. Dotani, K. Hayashida, H. Inoue, H. Kondo, K. Koyama, K. Mitsuda, Y. Ogawara, S. Takano, H. Awaki, Y. Tawara, and N. Nakamura, 1989, PASJ 41, 345

Turner, M. J. L., O. R. Williams, T. J.-L. Courvoisier, G. C. Stewart, K. Nandra, K. A. Pounds, T. Ohashi, K. Makishima, H. Inoue, T. Kii, F. Makino, K. Hayashida, Y. Tanaka, S. Takano, and K. Koyama, 1990, MNRAS 244, 310

Ulrich, M.-H., 1981, Sp. Sci. Rev. 28, 89

Ulrich, M.-H, T. J.-L. Courvoisier, and W. Wamstecker, 1988, A&A 204, 21

Walter, R., and T. J.-L. Courvoisier, 1992, A&A 258, 255

Williams, O. R., K. Bennett, J. B. G. Bloemen, W. Collmar, R. Diehl, W. Hermsen, G. G. Lichti, M. McConnell, D. Morris, R. Much, J. Ryan, V. Schönfelder, H. Steinle, and A. W. Strong, 1994, accepted for publication in A&A

Zbyszewska, M., 1993, AIP Conf. Proc. 280, 608

Zdiarski, A. A., G. Ghisellini, I. M. George, R. Svensson, A. C. Fabian, and C. Done, 1990, ApJ 363, L1

This article was processed by the author using Springer-Verlag TEX A&A macro package 1992.